

Catalysis of the Electro-Oxidation of Carbon Monoxide by Cobalt Octaethylporphyrin

Chunnian Shi and Fred C. Anson*

Arthur Amos Noyes Laboratories, Division of Chemistry and Chemical Engineering,
California Institute of Technology, Pasadena, California 91125

Received May 21, 2001

The electro-oxidation of cobalt (II) octaethylporphyrin adsorbed on graphite electrodes, $\text{Co}^{\text{II}}(\text{OEP})_{\text{ads}}$ to $\text{Co}^{\text{III}}(\text{OEP})_{\text{ads}}^+$, in the presence of aqueous solutions of CO leads to catalytic oxidation of CO to CO_2 . No such oxidation occurs with $\text{Co}^{\text{II}}(\text{OEP})$ and CO dissolved in nonaqueous solvents. Coordination of the CO to $\text{Co}^{\text{III}}(\text{OEP})^+$ is the first step in the catalytic mechanism. Nucleophilic attack on the coordinated CO by H_2O is the probable rate-limiting step in the catalytic oxidation. A pseudo first-order rate constant of 0.3 s^{-1} was estimated for this reaction.

Introduction

Kadish and co-workers have demonstrated that, in nonaqueous solvents, cobalt porphyrins exhibit a high affinity for CO in their Co(III) but not their Co(II) oxidation states.^{1–3} This somewhat surprising observation stimulated our interest in determining if the coordination of CO to Co(III) porphyrins could also be observed in aqueous media and, if so, whether the coordinated CO might be activated toward electrochemical oxidation. We chose to examine the effect of CO on the behavior of cobalt octaethylporphyrin, Co(OEP), because previous studies have shown that this molecule yields one of the clearest cyclic voltammetric responses when adsorbed on the surface of graphite electrodes, and the axial coordination sites of the cobalt center of the adsorbed porphyrin are accessible to ligands present in aqueous supporting electrolyte solutions.⁴ The results show that adsorbed Co(OEP) is an effective catalyst for the electro-oxidation of CO. Mechanistic aspects of the catalytic process and the rate constant for the current-limiting step are described in this report.

Experimental Section

Materials. Cobalt octaethylporphyrin (Aldrich) was purified by passage through a column of activated basic alumina (150 mesh, 58 Å, Aldrich) using chloroform as the eluent. CHCl_3 (EM Science, Omni Solv) was passed through a similar column of alumina just prior to its use. Laboratory distilled water was further purified by passage through a purification train (Milli-Q Plus from Millipore). Other chemicals were reagent grade and used as received. The pH of supporting electrolyte solutions was controlled by Britton-Robinson buffers between pH 3 and 12. Below pH 3, HClO_4 was used to adjust the concentration of protons in $\text{NaClO}_4\text{--HClO}_4$ mixtures maintained at unit ionic strength.

Apparatus and Procedures. Conventional electrochemical instrumentation and two-compartment cells were employed. Pyrolytic graphite rods (Advanced Ceramics Corp.) were used to construct the working electrodes. Cylindrical segments were mounted on stainless steel shafts

with heat-shrinkable tubing (Alpha Wire Co.), leaving 0.32 cm^2 of the edges of the graphite planes exposed to the solution. Before each experiment, the electrode surface was rough polished with 600 grit SiC paper, sonicated in pure water, and dried in air with a heat gun. The counter electrode was a coil of platinum wire, and a commercial saturated calomel electrode served as the reference electrode.

Co(OEP) was adsorbed on the freshly polished electrode surface by dipping it for 10 s in a solution of the porphyrin in CHCl_3 followed by washing with pure solvent. With 0.5 mM solutions of the porphyrin, this procedure typically resulted in the irreversible adsorption of ca. $8 \times 10^{-10} \text{ mole cm}^{-2}$ of Co(OEP), as determined by coulometric assays based on the areas under cyclic voltammetric peaks recorded at scan rates of 50 mV s^{-1} or less. To obtain smaller quantities of adsorbed porphyrin, more dilute solutions were employed. Potentials were measured and are reported with respect to a saturated calomel reference electrode. Experiments were conducted at ambient laboratory temperatures, $22 \pm 2 \text{ }^\circ\text{C}$.

Results

Effect of CO on the Electrochemistry of Adsorbed Co(OEP). The coordination of CO to $\text{Co}^{\text{III}}(\text{OEP})^+$ dissolved in CH_2Cl_2 is well established.^{2,5} Under CO, the $(\text{OC})\text{Co}^{\text{III}}(\text{OEP})^+$ complex is stable, and its electro-oxidation causes simple dissociation of the CO as $\text{Co}(\text{OEP})^{2+}$ is formed.² In the presence of competing axial ligands, such as nitriles, the coordination of CO to $\text{Co}^{\text{III}}(\text{OEP})^+$ is expected to become less extensive;¹ in aqueous solutions, the ability of $\text{Co}^{\text{III}}(\text{OEP})^+$ adsorbed on graphite electrodes to coordinate CO instead of H_2O was uncertain. To determine if CO coordination occurred, the system was examined initially by means of cyclic voltammetry.

Shown in Figure 1A are the essentially featureless cyclic voltammetric responses obtained from EPG electrodes in argon-saturated aqueous solutions at three pH values. When the solutions were saturated with CO there were no changes in the responses, which showed that no direct electro-oxidation of CO occurred in the range of potentials of interest. The dashed curves in Figure 1B are the responses obtained when the experiments were repeated under Ar, but with $\text{Co}^{\text{II}}(\text{OEP})$ irreversibly adsorbed on the EPG electrode. The reversible responses correspond to the $\text{Co}^{\text{III}}/\text{Co}^{\text{II}}$ couple of the adsorbed Co(OEP).⁴ The area under the peaks corresponds to ca. $8 \times 10^{-10} \text{ mole}$

* To whom correspondence should be addressed. E-mail: fanson@caltech.edu. Telephone: (626) 395-6000. FAX: (626) 577-4088.

(1) Mu, X. H.; Kadish, K. M. *Inorg. Chem.* **1989**, *28*, 3743–3747.

(2) Hu, Y.; Han, B. C.; Bao, L. Y.; Mu, X. H.; Kadish, K. M. *Inorg. Chem.* **1991**, *30*, 2444–2446.

(3) Kadish, K. M.; Li, J.; Van Caemelbecke, E.; Ou, Z.; Guo, N.; Autret, M.; D'Souza, F.; Tagliatesta, P. *Inorg. Chem.* **1997**, *36*, 6292–6298.

(4) Song, E.; Shi, C.; Anson, F. C. *Langmuir* **1998**, *14*, 4315–4321.

(5) Schmidt, E.; Zhang, H.; Chang, C. K.; Babcock, G. T.; Oertling, W. *A. J. Am. Chem. Soc.* **1996**, *118*, 2954–2961.

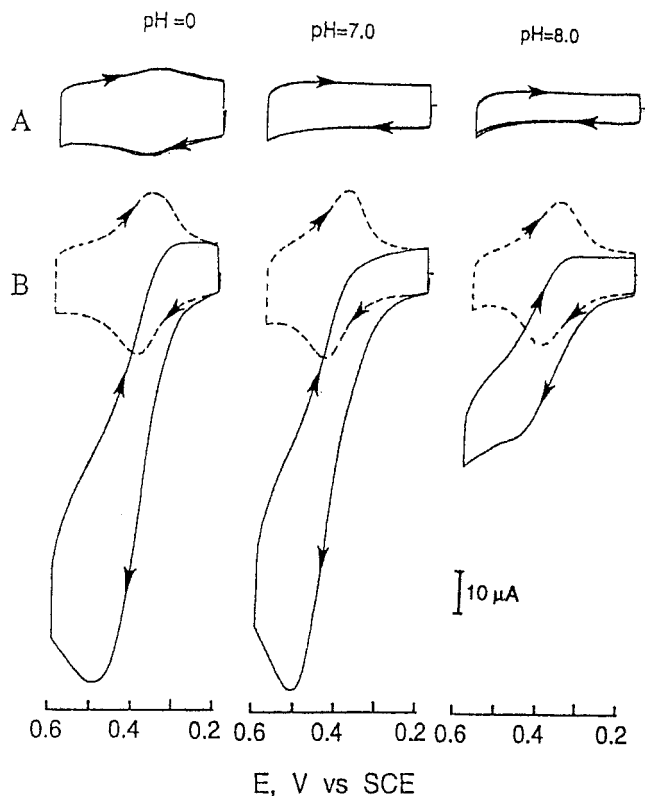


Figure 1. Cyclic voltammograms demonstrating the catalytic activity of adsorbed Co(OEP) toward the electro-oxidation of CO. (A) Bare EPG electrode in the absence and presence of CO (the two curves are indistinguishable) at the indicated pH values. (B) Dashed curves: repeat of (A) under Ar after $\sim 8 \times 10^{-10}$ mole cm^{-2} of Co(OEP) was adsorbed on the EPG electrode. Solid curve: with the solution saturated with CO. Supporting electrolytes: 1M HClO₄ or 1M NaClO₄ + 10 mM Britton–Robinson buffers. Scan rate: 50 mV s⁻¹.

cm^{-2} of adsorbed, electroactive Co(OEP) on the surface. The solid curves in Figure 1B were recorded after the supporting electrolytes were saturated with CO. The large anodic peak currents at pH 0 and 7, and the smaller current at pH 8, must arise from the anodic oxidation of CO catalyzed by the adsorbed Co(OEP). The rise in the catalytic currents occurs at the same potential where, in the absence of CO, the adsorbed Co^{II}(OEP) is oxidized to Co^{III}(OEP)⁺, which implicates the oxidized porphyrin as the catalytically active species.

The magnitude of the peak currents in Figure 1B at pH 0 and 7 (after subtraction of the contribution from the adsorbed Co^{II}(OEP)) are about half as large as the calculated diffusion-limited current for the two-electron irreversible oxidation of CO. Thus, the catalytic current is probably limited by the rate of a chemical step preceding the electrode reaction.

pH Dependence. The catalytic currents for the electro-oxidation of CO (as catalyzed by adsorbed Co^{III}(OEP)⁺) are unaffected by changes in pH between pH 0 and 7. At pH 8, the current is significantly diminished (Figure 1B), and at higher pH values the electro-oxidation is much slower. To examine this behavior, the pH dependence of the formal potentials of the adsorbed Co^{III}(OEP)⁺/Co^{II}(OEP) couple were evaluated from the average of the anodic and cathodic peak potentials of voltammograms such as the dashed curves in Figure 1. The results are shown in Figure 2. Between pH 0 and 7, the formal potentials are essentially constant. Above pH 7 the values of E^f decrease by 59 mV per pH unit, as expected if one proton were consumed during the reduction of Co^{III}(OEP)⁺ in this pH range. This behavior can be understood if a water molecule occupying

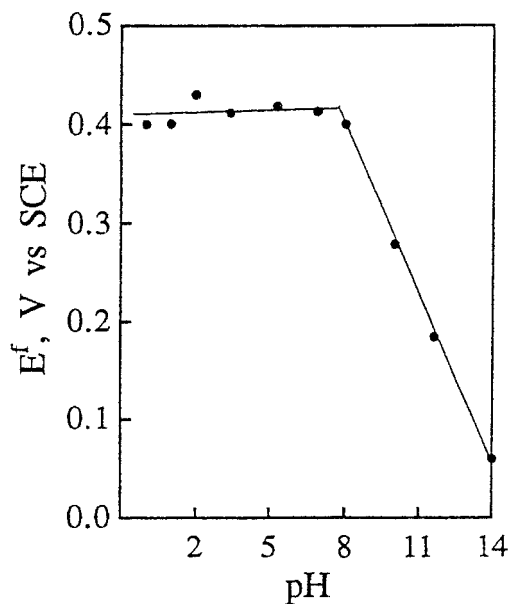
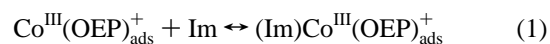


Figure 2. Formal potentials of the Co^{III}(OEP)⁺/Co^{II}(OEP) couple adsorbed on EPG electrodes as a function of the pH of the aqueous supporting electrolyte. pH values were established with 10 mM Britton–Robinson buffers added to 1 M NaClO₄; at pH values below 3, NaClO₄–HClO₄ mixtures were employed at constant ionic strength (1 M).

an axial site on the Co(III) center had a pK_a near 8, while on the Co(II) center the pK_a were greater than 14.

The behavior shown in Figure 2 provides a reasonable explanation for the pH dependence of the catalyzed electro-oxidation of CO; at pH values less than 8, CO molecules that coordinate to the cobalt center of adsorbed Co^{III}(OEP)⁺ compete with H₂O molecules for the coordination site, but at higher pH values the CO must compete with more strongly bound OH⁻ ligands, which may prevent its coordination (and activation toward electro-oxidation).

Hydroxide is not the only ligand that interferes with the coordination of CO to adsorbed Co^{III}(OEP)⁺. Both pyrazine and imidazole act similarly, as shown in Figure S1 (Supporting Information). The coordination of the latter ligand at pH 7 is so strong that the formal potential of the Co(III/II) couple is shifted to considerably more negative values, and the quantity of unoccupied axial coordination sites on the adsorbed Co^{III}(OEP)⁺ is too small to yield any detectable oxidation of CO at the potential where the oxidation of Co^{II}(OEP) occurs or at the more positive potentials, where the oxidation of CO was observed in Figure 1. Shown in Figure S2 (Supporting Information) is the change in the formal potential of the Co(III/II) couple with the concentration of imidazole, Im. The slope of the line, 58 mV per decadic change in [Im], indicates that a single Im ligand coordinates to the adsorbed Co^{III}(OEP)⁺. The -0.32 V shift in E^f produced by the presence of 1 mM Im corresponds to an equilibrium constant of 3×10^8 M⁻¹ for reaction 1.



The second axial coordination site of the adsorbed porphyrin is apparently inaccessible, as would be expected if the Co(OEP) is adsorbed with the porphyrin ring parallel to the graphite surface. Similar behavior was reported in a previous study of adsorbed cobalt tetramethylporphyrin.⁶

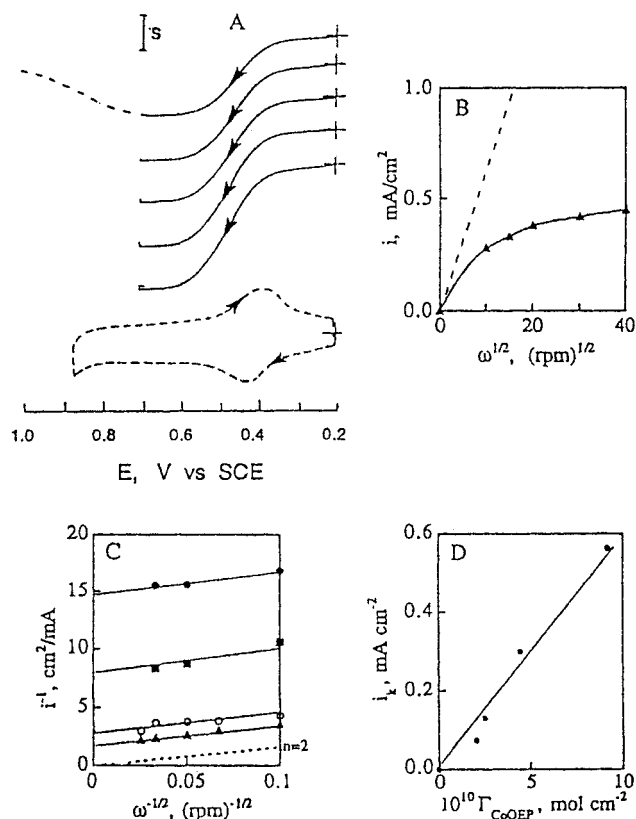


Figure 3. (A) Current–potential curves for the electro-oxidation of CO at a rotating pyrolytic graphite disk electrode on which $\sim 9 \times 10^{-10}$ mole cm^{-2} of Co(OEP) had been adsorbed. Supporting electrolyte: 1 M HClO_4 saturated with CO. Electrode rotation rates (from top to bottom) 100, 225, 400, 900, and 1600 rpm. Potential scanned at 10 mV s^{-1} , $S = 50 \mu\text{A}$. The dashed portion of the uppermost curve shows the decrease in current that occurs at potentials more positive than 0.7 V. The dashed cyclic voltammogram at the bottom was recorded in the absence of CO at a scan rate of 50 mV s^{-1} , $S = 20 \mu\text{A}$. (B) Levich plot of the plateau currents in (A) versus the electrode (rotation rate) $^{1/2}$. The dashed line is the calculated response for the diffusion-convection-limited two-electron oxidation of CO using $D_{\text{CO}} = 2.1 \times 10^{-5} \text{ cm}^2 \text{ s}^{-1}$ and $[\text{CO}] = 1 \text{ mM}$ in solutions saturated with CO at 1 atm. 10 (C) Koutecky–Levich plots of data like those in (B) obtained with increasing quantities of adsorbed Co(OEP), $\Gamma_{\text{Co(OEP)}} = 2.0 \times 10^{-10}$ (●), 2.5×10^{-10} (■), 4.5×10^{-10} (○), and 9.2×10^{-10} mole cm^{-2} (▲). (D) Dependence of the kinetic currents, i_k , (obtained from the intercepts of the plots in (C)) on $\Gamma_{\text{Co(OEP)}}$.

Kinetics of the Oxidation of CO. To obtain quantitative data on the rate of the catalyzed electro-oxidation of CO, experiments were conducted with the Co(OEP) catalyst adsorbed on a rotating graphite disk electrode. Current–potential curves obtained in such experiments are shown in Figure 3A along with the cyclic voltammetric response from the adsorbed catalyst in the absence of CO (dashed curve).

For the uppermost current–potential curve in Figure 3A, the electrode potential was scanned to values beyond the current plateau, which caused the catalytic current to decrease substantially. This behavior is likely to be the result of oxidation of $\text{Co}^{\text{III}}(\text{OEP})^+$ to $\text{Co}^{\text{III}}(\text{OEP}^+)_2^+$ (OEP^+ is the radical cation produced by the oxidation of the OEP ligand), because the latter complex was shown by Kadish et al. not to coordinate CO. 2 No clear response attributable to the $\text{Co}^{\text{III}}(\text{OEP})^{2+}/\text{Co}^{\text{III}}(\text{OEP})^+$ couple was observed in cyclic voltammograms, probably because the oxidized OEP $^+$ cation is unstable in the presence of water. The noteworthy point about Figure 3A is the demonstration that the catalytic activity toward CO oxidation

is restricted to $\text{Co}^{\text{III}}(\text{OEP})^+$, which is also the only oxidation state of the porphyrin that coordinates CO. 2

The anodic plateau currents of Figure 3A were used to prepare the Levich plot 7 in Figure 3B. The nonlinearity of the plot with currents that fall well below the line calculated for the diffusion-convection-limited oxidation of CO to CO_2 (dashed line) is a sign that the magnitude of the plateau currents is controlled by a chemical step preceding the electrode reaction. Data like those in Figure 3B were analyzed by means of Koutecky–Levich plots, 8 as shown in Figure 3C for experiments with varying quantities of Co(OEP) adsorbed on the rotating graphite disk electrode. The slopes of the plots match that calculated for the two-electron oxidation of CO (dashed line), and the intercepts were used to calculate kinetic currents, i_k , that measure the rate of the current-limiting chemical reaction. 9 The resulting values of i_k are plotted versus the quantity of Co(OEP) on the electrode, $\Gamma_{\text{Co(OEP)}}$, in Figure 3D. The linearity of the plots in Figure 3C and D indicates that the rate of the current-limiting reaction is first order in both CO and $\Gamma_{\text{Co(OEP)}}$.

Under these conditions, i_k is given by eq 2

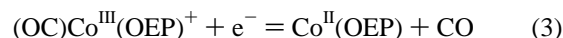
$$i_k = 2kFAC_{\text{CO}}\Gamma_{\text{Co(OEP)}} \quad (2)$$

where k is the second-order rate constant governing the current-limiting reaction, F is the Faraday, A is the electrode area, and C_{CO} is the concentration of CO in the solution (1.0 mM at 1 atm 10). The value of k obtained from the slope of the line in Figure 3D is $3 \times 10^3 \text{ M}^{-1} \text{ s}^{-1}$.

The data in Figure 3 were obtained with 1 M HClO_4 as the supporting electrolyte. Essentially similar results were obtained using 0.1 M HClO_4 –0.9 M NaClO_4 and 0.01 M HClO_4 –0.99 M NaClO_4 as supporting electrolytes. Thus, the reaction rate is independent of $[\text{H}^+]$.

Discussion

Comparison with Results in Nonaqueous Solvents. The voltammograms shown in Figure 1B are very different from those obtained with solutions of Co $^{\text{II}}$ (OEP) and CO in solvents such as CH_2Cl_2 . 2 In the absence of CO, the first oxidation of Co $^{\text{II}}$ (OEP) produces Co $^{\text{II}}$ (OEP $^+$) instead of Co $^{\text{III}}$ (OEP $^+$). 1,2 In the presence of CO the oxidation follows a different course and produces (OC)Co $^{\text{III}}$ (OEP) $^+$ and (OC) $_2$ Co $^{\text{III}}$ (OEP) $^+$, which are stable complexes that can be reduced to Co $^{\text{II}}$ (OEP) and CO. There is no evidence for oxidation of the coordinated CO in nonaqueous solvents. However, as shown in Figure 1B, the oxidation of CO commences as soon as Co $^{\text{II}}$ (OEP) $_{\text{ads}}$ is oxidized to Co $^{\text{III}}$ (OEP) $_{\text{ads}}^+$ in aqueous solutions so that the response from half-reaction 3,



which is readily observed in nonaqueous solvents, 2 is not observable in aqueous media. In the absence of a source for the oxygen that is needed for the conversion of CO to CO_2 , the coordination of CO to Co $^{\text{III}}$ (OEP) $^+$ does not facilitate the oxidation of CO. In the presence of an oxygen source (H_2O) the coordinated CO is activated to such an extent that its electro-

(7) Levich, V. G. *Physicochemical Hydrodynamics*; Prentice Hall: Englewood Cliffs, NJ, 1962.

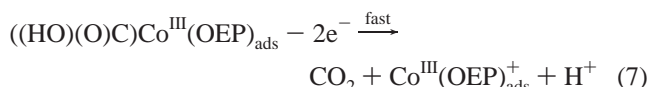
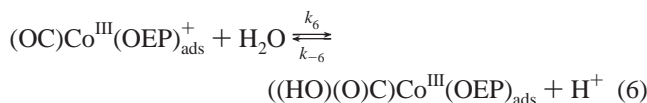
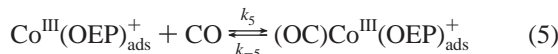
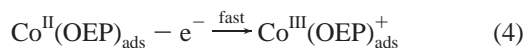
(8) Koutecky, J.; Levich, V. G. *Zh. Fiz. Khim.* **1956**, *32*, 1565.

(9) Andrieux, C. P.; Saveant, J.-M. *J. Electroanal. Chem.* **1982**, *134*, 163–166.

(10) Napporn, W. T.; Léger, J.-M.; Lamy, C. *J. Electroanal. Chem.* **1996**, *408*, 141–147.

oxidation accompanies the oxidation of $\text{Co}^{\text{II}}(\text{OEP})_{\text{ads}}$. That is, the potential where the coordinated CO can be oxidized is less positive than that where $\text{Co}^{\text{II}}(\text{OEP})_{\text{ads}}$ is oxidized to $\text{Co}^{\text{III}}(\text{OEP})_{\text{ads}}^+$.

Mechanism. The available data are consistent with the overall reaction mechanism given in reactions 4–7.



Half-reactions 4 and 7 proceed rapidly at potentials on the plateaus of the current–potential curves in Figure 3A. The magnitudes of the plateau currents could be limited by the rate of coordination of CO to $\text{Co}^{\text{III}}(\text{OEP})_{\text{ads}}^+$ (reaction 5) or by the rate of the conversion of the coordinated CO into a more readily oxidizable form (reaction 6). (There is no direct evidence for the hydroxylated CO that is depicted as the product of reaction 6, but it has been suggested previously to be the oxidizable species that results from the reaction of H_2O with CO coordinated to a Rh(III) halide complex¹¹ and to Rh(III) and Ir(III) porphyrins.^{12,13}) Rate constants governing the coordination of O_2 to Co(II) porphyrins adsorbed on graphite are typically 10^4 – $10^5 \text{ M}^{-1} \text{ s}^{-1}$ ¹⁴ in aqueous solutions, although the equilibrium constant for the coordination reaction is less than 1 M^{-1} . The equilibrium constant for the coordination of CO to $\text{Co}^{\text{III}}(\text{OEP})^+$ (in CH_2Cl_2) is much larger, $\sim 1.6 \times 10^4 \text{ M}^{-1}$,^{1,5} so that one would anticipate a rate constant for the coordination reaction that was larger than the 10^4 – $10^5 \text{ M}^{-1} \text{ s}^{-1}$ values that are observed for the coordination of O_2 to Co(II) porphyrin. Since the rate constant obtained from the slope of the line in Figure 3D is only $3 \times 10^3 \text{ M}^{-1} \text{ s}^{-1}$, the reaction to which it applies is unlikely to be reaction 5. Instead, reaction 6 is the more likely current-limiting reaction, with reaction 5 remaining at equilibrium. In that case, the rate constant obtained from Figure 3D would be a composite product, $k = 3 \times 10^3 \text{ M}^{-1} \text{ s}^{-1} = K_5 k_6$, where K_5 is the equilibrium constant of reaction 5, k_6 is the pseudo first-order rate constant for the reaction of $(\text{OC})\text{Co}^{\text{III}}(\text{OEP})^+$ with the solvent (H_2O), and reaction 6 is regarded as irreversible because of the rapid consumption of its product in reaction 7. If K_5 is taken to be $\sim 10^4 \text{ M}^{-1}$ on the basis of its value in CH_2Cl_2 ,^{1,5} the calculated value of k_6 is $3 \times 10^{-1} \text{ s}^{-1}$.

A conceivable alternative mechanism in which coordination of CO to $\text{Co}^{\text{II}}(\text{OEP})$ preceded the oxidation of the Co(II) center is unlikely because of the negligible affinity of the unoxidized porphyrin for CO^{1,2} and the close correlation between the reversible potential of the $\text{Co}^{\text{III}}(\text{OEP})_{\text{ads}}^+/\text{Co}^{\text{II}}(\text{OEP})_{\text{ads}}$ couple and the potential at which the oxidation of CO occurs.

The coordination of CO by $\text{Co}^{\text{III}}(\text{OEP})^+$, but not by $\text{Co}^{\text{II}}(\text{OEP})$ or by $[\text{Co}^{\text{III}}(\text{OEP}^+)]^{2+}$,² is somewhat surprising. One could imagine that the attachment of the CO to the metal center depended upon back-bonding interactions that involved the electrons in the π system of the porphyrin ring. However, on the basis of IR spectroscopic experiments, Schmidt et al.⁵ have argued that the bonding of CO to $\text{Co}^{\text{III}}(\text{OEP})^+$ occurs primarily as a result of ligand–to–metal σ donation instead of the π back donation that is the most common mode of bonding CO to low valent metal centers. This interpretation is consistent with the lack of coordination of CO to the less electrophilic $\text{Co}^{\text{II}}(\text{OEP})$ (although the reason for the instability of $[(\text{OC})\text{Co}^{\text{III}}(\text{OEP}^+)]^{2+}$ is not explained). Such σ donation from CO to Co(III) is also consistent with the more facile electro-oxidation of the coordinated CO. Enhancement of the positive character of the coordinated CO resulting from its σ donation would facilitate nucleophilic attack by H_2O (reaction 6) to yield a species well disposed to transfer electrons to the electrode to produce CO_2 , which has little affinity for the Co(III) center, and a catalytic cycle ensues. Thus, the unusual ability of $\text{Co}^{\text{III}}(\text{OEP})^+$ to catalyze the electro-oxidation of CO may be attributed to the equally unusual ability of this complex to form complexes with CO that involve primarily σ donation instead of π back donation.

Previous Reports of Electrocatalytic Oxidation of CO. In pioneering studies of the use of adsorbed metal chelates as catalysts for the electro-oxidation of CO, van Baar et al. found that Ir, Rh, and Co tetraphenylporphyrins were effective catalysts when adsorbed on high area carbon electrodes.^{12,13} Their speculations about possible mechanisms for the catalysis also invoked nucleophilic attack by water on CO coordinated to the metal centers. A protonation step that preceded a rate-determining electron-transfer step was also proposed, but the independence of the catalytic rate on pH between pH 0 and 7, as observed in the present study, casts doubt on this aspect of the mechanism. However, the electrode material, pretreatment procedures, and supporting electrolytes (8 M H_2SO_4 , 6 M KOH) employed by van Baar et al.^{12,13} were very different from those in the present study, so the catalytic mechanisms encountered in the two studies might also be dissimilar.

Wu and Kubiak¹⁵ described a system for the electro-oxidation of CO to CO_2 based on a homogeneous catalyst, $[\text{Rh}(\text{CO})_2\text{Br}_2]^-$, that was cycled between oxidation states at a glassy carbon electrode. Nucleophilic attack on coordinated CO was also invoked in this study to account for the catalysis, but the current-limiting step was not identified.

Conclusions

The reversible coordination of CO by Co(III) porphyrins, e.g., $\text{Co}^{\text{III}}(\text{OEP})^+$, dissolved in nonaqueous solvents, as demonstrated by Kadish and co-workers,^{1,2} produces stable complexes that release the coordinated CO intact upon either oxidation or reduction. However, when the $\text{Co}^{\text{III}}(\text{OEP})^+$ is generated by the oxidation of $\text{Co}^{\text{II}}(\text{OEP})$ adsorbed on graphite electrodes in aqueous solutions in the presence of CO, an immediate catalytic electro-oxidation of CO to CO_2 ensues. The coordination of the CO to the oxidized porphyrin followed by its electro-oxidation could not be observed as separate steps because the coordinated CO is oxidized at potentials no more positive than that where the coordinating $\text{Co}^{\text{III}}(\text{OEP})^+$ is produced. The rate-limiting step in the catalytic mechanism is believed to be the conversion of the coordinated CO to a more readily oxidized species by nucleophilic attack by H_2O . For the case of $(\text{OC})\text{Co}^{\text{III}}(\text{OEP})^+$

- (11) Cheng, C.-H.; Hendriksen, D. E.; Eisenberg, R. *J. Am. Chem. Soc.* **1977**, *99*, 2971–2972.
 (12) Van Baar, J. F.; van Veen, J. A. R.; de Wit, N. *Electrochim. Acta* **1982**, *27*, 57–59.
 (13) Van Baar, J. F.; van Veen, J. A. R.; van der Eijk, J. M.; Peters, Th. J.; de Wit, N. *Electrochim. Acta* **1982**, *27*, 1315–1319.
 (14) Shi, C.; Anson, F. C. *Inorg. Chim. Acta* **1994**, *225*, 215–227.

- (15) Wu, J.; Kubiak, C. P. *J. Am. Chem. Soc.* **1983**, *105*, 7456–7457.

adsorbed on pyrolytic graphite, the pseudo first-order rate constant governing this reaction was estimated as $\sim 3 \times 10^{-1} \text{ s}^{-1}$.

Acknowledgment. This work was supported by the National Science Foundation. We are grateful to Prof. Karl Kadish for calling our attention to the reaction between Co(III) porphyrins and CO.

Supporting Information Available: Two figures showing cyclic voltammograms for Co(OEP) in the presence of pyrazine or imidazole with and without CO and the variation in the formal potential of the Co(III/II) couple with the concentration of imidazole (PDF). The material is available free of charge via the Internet at <http://pubs.acs.org>.

IC010530B